Influence of the processing on composition, protein structure and techno-functional properties of mealworm protein concentrates produced by isoelectric precipitation and ultrafiltration/diafiltration

Pinel, Gwenn; Berthelot, Ugo; Queiroz, Lucas Sales; Santiago, Livia De Almeida; Silva, Naaman Francisco Nogueira; Petersen, Heidi Olander; Sloth, Jens J.; Altay, Ipek; Marie, Rodolphe; Feyissa, Aberham Hailu

Total number of authors:
12

Published in:
Food Chemistry

Link to article, DOI:
10.1016/j.foodchem.2024.139177

Publication date:
2024

Document Version
Publisher's PDF, also known as Version of record

Food Chemistry 449 (2024) 139177

Contents lists available at ScienceDirect

Food Chemistry

journal homepage: www.elsevier.com/locate/foodchem

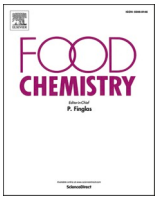

Influence of the processing on composition, protein structure and techno-functional properties of mealworm protein concentrates produced by isoelectric precipitation and ultrafiltration/diafiltration

Gwenn Pinel [a,b], Ugo Berthelot [a], Lucas Sales Queiroz [b], Livia De Almeida Santiago [b,c], Naaman Francisco Nogueira Silva [b,d], Heidi Olander Petersen [b], Jens J. Sloth [e], Ipek Altay [b], Rodolphe Marie [f], Aberham Hailu Feyissa [b], Federico Casanova [b,*], Alain Doyen [a,*]

[a] Department of Food Sciences, Institute of Nutrition and Functional Foods (INAF), Université Laval, Quebec City, QC G1V 0A6, Canada
[b] Research Group for Food Production Engineering, National Food Institute, Technical University of Denmark, Søltofts Plads, 2800 Kongens Lyngby, Denmark
[c] School of Food Engineering, University of Campinas, Campinas, São Paulo, Brazil
[d] Center of Natural Sciences, Federal University of São Carlos (UFSCar), Buri, 18290-000 São Paulo, Brazil
[e] Research Group for Analytical Food Chemistry, Technical University of Denmark, Kemitorvet, 2800 Kongens Lyngby, Denmark
[f] Department of Health Technology, Technical University of Denmark, Ørsted Plads, 2800 Kongens Lyngby, Denmark

ARTICLE INFO

Keywords:
Tenebrio molitor
Protein concentrate
Isoelectric precipitation
Ultrafiltration-diafiltration
Techno-functional properties

ABSTRACT

Edible insects represent a great alternative protein source but food neophobia remains the main barrier to consumption. However, the incorporation of insects as protein-rich ingredients, such as protein concentrates, could increase acceptance. In this study, two methods, isoelectric precipitation and ultrafiltration-diafiltration, were applied to produce mealworm protein concentrates, which were compared in terms of composition, protein structure and techno-functional properties. The results showed that the protein content of the isoelectric precipitation concentrate was higher than ultrafiltration-diafiltration (80 *versus* 72%) but ash (1.91 *versus* 3.82%) and soluble sugar (1.43 *versus* 8.22%) contents were lower. Moreover, the protein structure was affected by the processing method, where the ultrafiltration-diafiltration concentrate exhibited a higher surface hydrophobicity (493.5 *versus* 106.78 a.u) and a lower denaturation temperature (161.32 *versus* 181.44 °C). Finally, the ultrafiltration-diafiltration concentrate exhibited higher solubility (87 *versus* 41%) and emulsifying properties at pH 7 compared to the concentrate obtained by isoelectric precipitation.

1. Introduction

It is anticipated that the world demand for traditional animal-derived proteins (meat, dairy and egg), will double by 2050 (Henchion et al., 2017). It is well-documented that livestock production, particularly beef and pork, has major environmental repercussions, including global greenhouse gas emissions, deterioration of water and soil quality, and substantial demands on land, water, and energy resources (Dobermann et al., 2017). Therefore, the utilisation of alternative and sustainable protein sources will become more crucial (Van Huis et al., 2013). Edible insects have been identified as an emerging protein source due to their environmental, social and nutritional benefits (Gravel et al., 2021; Van Huis et al., 2013). Indeed, insects have a higher feed conversion efficiency than beef and pork, *i.e.* they require less feed

Abbreviations: IEP, isoelectric precipitation; UFDF, ultrafiltration-diafiltration; SIEP, supernatant from isoelectric precipitation; PUFDF, permeate from ultrafiltration-diafiltration; *T. molitor*, *Tenebrio molitor*; TMM, *T. molitor* meals; SDS-PAGE, sodium dodecyl sulfate-polyacrylamide gel electrophoresis; RFU, relative fluorescence units; ANS, 8-anilino-1-naphthalene sulfonate; H_0, hydrophobicity index; DSC, differential scanning calorimetry; FTIR, Fourier transform infrared spectroscopy; FC, foaming capacity; FS, foam stability; LGC, least gelling concentration; TSI, Turbiscan stability index; BS, backscattered signals; T, transmitted signals; CLSM, confocal laser scanning microscopy; ANOVA, one-way analysis of variance; MW, molecular weight; T_g, glass transition; T_u, thermal unfolding; T_m, solid-melting..

* Corresponding authors.
E-mail addresses: gwenn.pinel.1@ulaval.ca (G. Pinel), ugo.berthelot.1@ulaval.ca (U. Berthelot), lusaqu@food.dtu.dk (L.S. Queiroz), ldalsa@food.dtu.dk (L.D.A. Santiago), naaman.nogueira@ufscar.br (N.F.N. Silva), hope@food.dtu.dk (H.O. Petersen), jjsl@food.dtu.dk (J.J. Sloth), ipeal@food.dtu.dk (I. Altay), rcwm@dtu.dk (R. Marie), abhfe@food.dtu.dk (A.H. Feyissa), feca@food.dtu.dk (F. Casanova), alain.doyen@fsaa.ulaval.ca (A. Doyen).

https://doi.org/10.1016/j.foodchem.2024.139177
Received 15 November 2023; Received in revised form 15 March 2024; Accepted 27 March 2024
Available online 2 April 2024

to produce 1 kg of biomass (Rumpold & Schlüter, 2013; Van Broekhoven et al., 2015). Van Broekhoven et al. (2015) reported that the feed conversion ratio (amount of feed needed (kg) to obtain 1 kg of weight increase) of mealworms ranges between 2.5 and 3.5 depending on species and protein-rich diet, compared to 4.0 for pork and 8.8 for cereal beef (Wilkinson, 2011). In addition, insect rearing also requires less land and water use compared to conventional livestock. More specifically, Dobermann et al. (2017) reported that, to produce 1 kg of live animal weight, insects use on average 6 times less land, 5 times less feed and almost 4 times less water than beef. In terms of nutritional benefits, globally, insects are a good source of energy, proteins, fat, minerals and vitamines, (Dobermann et al., 2017). More specifically, insects have a high protein content that includes all the essential amino acids, making them comparable to more traditional protein sources (beef, chicken, and fish). Moreover, insect proteins are, on average, more digestible than plant-based proteins and slightly less digestible than animal-based ones (Dobermann et al., 2017). In particular, *Tenebrio molitor* (yellow mealworm) is proving to be of great interest due to its high protein content (Gravel et al., 2021; Van Huis et al., 2013). Nevertheless, consumer acceptance is notably low, particularly within Western culture. However, an interesting option to improve acceptance would be to avoid the visual appearance of insects in food products and promote the integration of insect-based ingredients in conventional food matrices (La Barbera et al., 2018).

Based on the methodology for producing plant-based protein isolates, various extraction methods can be used to produce insect protein concentrates and isolates, including aqueous extraction, salt extraction, alkaline solubilization, and acid precipitation (Gravel & Doyen, 2020). However, the most commonly used method remains alkaline solubilization, followed by isoelectric precipitation (IEP), since this combination generally results in higher extraction yields than those obtained by aqueous or salt extraction (Gravel & Doyen, 2020). Indeed, since mealworm proteins show maximum solubility at extreme pH values, alkaline solubilization provides a high protein recovery yield ($\geq$ 60%). Moreover, as mealworms contain mainly muscular proteins (such as tropomyosin, myosin, actin) (Leni et al., 2020), but also hemolymph proteins (hexamerin 1 and 2), cuticular proteins and enzymes (de Gier & Verhoeckx, 2018; Leni et al., 2020; Yi et al., 2016), alkaline solubilization is more efficient for extraction of myofibrillar proteins compared to aqueous extraction. However, despite its benefits in terms of protein extraction yield, IEP, which consists of adjusting the pH to the isoelectric point of proteins to promote protein-protein interactions and precipitation (Türker et al., 2022), presents certain disadvantages. In particular, IEP has a substantial ecological impact (water and energy consumption, effluent generation) (Laroche et al., 2022) and a negative impact on the native protein structure (Dill & Shortle, 1991). Ultrafiltration (UF)-diafiltration (DF) process is also of great interest to produce protein-rich insect ingredients (Gravel & Doyen, 2020). UF is a pressure-driven membrane process using semi-permeable membranes with molecular weight cut-offs ranging from 5 to 500 kDa for protein concentration in the retentate. Compared to IEP, the main advantage of UFDF is that proteins remain in their native state (Boye et al., 2010). DF, which consists of adding water to the concentrated retentate, is often combined with UF to increase protein purity in the retentate by the elimination of low molecular weight components such as sugar, salt and non-protein nitrogen (Doran, 2012). However, although UFDF is considered efficient, environmentally friendly, and economical, the main disadvantage of this method is membrane fouling (Gravel & Doyen, 2020). Consequently, the choice of using IEP or UFDF is crucial since it was demonstrated that the composition of protein isolates as well as protein structure and techno-functional properties were differently affected depending on the processing method. Indeed, the protein content of isolates was generally higher when utilising UFDF compared to IEP. In Kabuli chickpea, Boye et al. (2010) reported protein contents of 68.5 and 63.9% while Mondor et al. (2009) reported protein contents of 72.3 and 69.6% for UFDF and IEP, respectively. Moreover, the techno-functional properties (foaming, gelling and emulsifying) as well as the solubility of UFDF protein isolates were also better than those obtained after IEP (Lo et al., 2021). Recently, Berthelot et al. (2023) generated a mealworm protein concentrate by using UFDF and showed a high retention of proteins in the UF-retentate while the permeate was mainly composed of free amino acids and low molecular weight peptides. However, no comparative studies of composition, protein structure and techno-functional properties of mealworm protein concentrates produced by IEP and UFDF have been performed in the literature. In addition, to the best of our knowledge, only one study investigated the use of UFDF on mealworm meal (Ranasinghe et al., 2023). However, the objective of this work was to fractionate the different proteins and not to produce a protein concentrate. Therefore, the purpose of this work is to compare for the first time the proximate composition, protein profile and structure, and techno-functional properties of *T. molitor* protein concentrates produced by UFDF and IEP to identify potential applications for the biofood sector. Consequently, our hypothesis was that the production method (IEP *versus* UFDF) has an impact on the composition, protein structure, and techno-functional properties of a mealworm protein concentrate.

2. Material and methods

2.1. Chemicals

Hexane ($\geq$ 98.5% purity) was purchased from Thermo Fisher Scientific (Saint-Laurent, QC, Canada). Precision Plus Protein 1,610,373 All Blue Prestained Protein Standards, 12% TGX Stain-Free polyacrylamide gel, 2$\times$ Laemmli Sample buffer, and Coomassie Brilliant Blue R-250 used for protein profile observations were purchased from Bio-Rad (Mississauga, ON, Canada). 1-anilino-8-naphtalenesulfonate ($\geq$ 97% purity) was obtained from Sigma-Aldrich (Saint-Louis, MO, USA). Nile Red and FCF fast green dyes were acquired from Sigma-Aldrich (Denmark A/S, Søborg, Denmark). Tris HCl, sodium carbonate anhydrous, sodium bicarbonate, and sodium citrate used for buffer preparation were purchased from Sigma-Aldrich (Denmark A/S, Søborg, Denmark). All other reagents, solvents, acids, bases, and salts were purchased from Thermo Fisher Scientific, Sigma-Aldrich or *V*WR (Mont-Royal, QC, Canada).

2.2. Raw materials

Three batches of blanched (90 °C for 3 min) *T. molitor* larvae were obtained from Groupe Neoxis Inc. (Saint-Flavien, Quebec, Canada). Each batch was frozen at −30 °C, freeze-dried (pressure of 27 Pa and plate temperature of 20 °C) (REEP VirTis, SP Scientific, Warminster, PA, USA) and ground into a powder (Chopper 5KFC3515, KitchenAid, USA) to generate three different batches of *T. molitor* meals (TMM) which were stored at −30 °C for further analysis and experiments.

2.3. Production of mealworm protein concentrates

Mealworm protein concentrates were produced according to the protocol of Laroche et al. (2019) with a slight modification. Briefly, each TMM was suspended in deionised water at a ratio of 1:10 (*w/V*). The pH of the suspensions was adjusted to 11.0 using 5 M NaOH and maintained at this pH value for 1 h at 50 °C under continuous stirring. Afterwards, the suspensions were centrifuged (Avanti® JE Centrifuge, Beckman Coulter, Inc., CA, USA) at 8000 $\times g$ for 15 min at 4 °C and three phases were obtained. The top layer, which consisted of crystallized fat, was removed with a spatula. Then, the soluble (supernatant) and the insoluble (pellet) fractions were separated. A second centrifugation step (8000 $\times g$, 15 min, 4 °C) was applied to the supernatant to maximise the separation of the fat from the soluble phase. Proteins in the resulting supernatant were precipitated at pH 4.5 using 5 M HCl. The solution was then centrifuged at 8000 $\times g$ for 15 min at 20 °C and the pellet was recovered. To reduce the content of soluble compounds, the pellet was

washed with deionised water, the pH was adjusted to 4.5, and centrifuged at 8000 ×*g* for 10 min at 20 °C. This last step was repeated twice for a total of three wash steps. Finally, the pH of the pellet was neutralised to pH 7 using 1 M NaOH. All fractions – fat layer, pellet from alkaline extraction, supernatant from alkaline extraction, supernatant from IEP (SIEP), wash water as well as the IEP pellet *i.e.,* concentrate (IEP) – were frozen at −30 °C, freeze-dried (REEP VirTis, SP Scientific, Warminster, PA, USA), ground into powder, and stored at −30 °C for further analysis. The UFDF mealworm protein concentrate was the same as produced by Berthelot et al. (2023). The different steps to produce both concentrates are detailed in Fig. S1 of the supplementary material.

2.4. Protein extraction yield, proximate composition and mineral distribution

The protein extraction yield (from TMM to protein concentrate) and the protein process yield (from alkaline extraction supernatant to protein concentrate), were calculated according to Eqs. (1) and (2) (Laroche et al., 2019):

$$Protein\ extraction\ yield\ (\%) = \frac{m_C \times \%prot_C}{m_{TMM} \times \%prot_{TMM}} \times 100 \quad (1)$$

$$Protein\ process\ yield\ (\%) = \frac{m_C \times \%prot_C}{m_E \times \%prot_E} \times 100 \quad (2)$$

where m_C represents the mass (g) of the concentrate, m_{TMM} the mass (g) of the mealworm meal, m_E the mass (g) of mealworm protein extract obtained after alkaline solubilization; and $\%prot_C$, $\%prot_{TMM}$ and $\%prot_E$ represent the protein content of the concentrate, the mealworm meal, and the protein extract obtained after alkaline solubilization, respectively.

The proximate composition of TMM, IEP and UFDF concentrates, SIEP and UFDF permeate (PUFDF) were analysed in accordance with the protocols described below. The protein content was measured using the Dumas method (Elementar rapid Micro N cube, Langenselbold, Germany), with nitrogen-to-protein conversion factors of 6.25 for IEP and UFDF and 5.60 for SIEP and PUFDF (Janssen et al., 2017). The lipid content was determined using the Soxhlet method with hexane following the protocol of Laroche et al. (2019). Moisture and ash contents were determined using the official methods AOAC 950.46 (A) and AOAC 920.153, respectively. The soluble sugar content was obtained as described by Giannoccaro et al. (2006) with modifications. Briefly, 0.5 g of IEP and UFDF concentrates, SIEP and PUFDF were suspended in deionised water at a ratio of 1:80 (*w/V*) and stirred for 30 min at 22 °C. The suspension was then centrifuged at 18,000 ×*g* for 30 min at 20 °C (Avanti® JE Centrifuge, Beckman Coulter, Inc., CA, USA) and the supernatant was collected. One millilitre of the supernatant was then mixed with 1 mL of a 5% (*w/V*) phenol solution and 5 mL of H_2SO_4. After 30 min, the UV-absorbance of the mixture was read at 487 nm with a UV–visible spectrometer (Fluoroskan Ascent® FL, Thermo Fisher Scientific, Saint-Laurent, QC, Canada) and the concentration of soluble sugars was determined from a standard curve of glucose. The mineral distribution was analysed by inductively coupled plasma mass spectrometry (Thermo iCAPq ICPMS, Thermo Electron, Bremen, Germany) following microwave-assisted digestion (Multiwave 7000, Anton Paar, Graz, Austria) using concentrated nitric acid.

2.5. Protein profile analysis by gel electrophoresis

The mealworm protein profiles of the four fractions of interest (IEP, UFDF, SIEP and PUFDF) were obtained using sodium dodecyl sulfate-polyacrylamide gel electrophoresis (SDS-PAGE) under non-reducing and reducing conditions. According to the method of Boukil et al. (2022) with a few modifications. Briefly, solutions containing 1% (*w/V*) of the different fractions were prepared. For the non-reducing conditions, 25 µL of each solution was combined with 25 µL of buffer (Laemmli 2 ×) (Bio-Rad, Mississauga, ON, Canada) and 10 µL of this mixture was loaded per well. For the reducing conditions, 25 µL of each solution was combined with buffer (5% 2-mercaptoethanol with 95% Laemmli 2 ×). The obtained solutions were immersed in boiling water for 5 min and then cooled on ice for 10 min before loading 10 µL per well. For both conditions, electrophoresis was performed on a 12% TGX Stain-Free polyacrylamide gel (Bio-Rad, Mississauga, ON, Canada) with a running buffer of 1 × tris-glycine SDS solution (Bio-Rad, Mississauga, ON, Canada) at 15 mA at 22 °C until the migration was complete. Coomassie blue (1 g/L of Coomassie Brilliant Blue R-250, 10% acetic acid, 40% ethanol and 50% water) was used to stain the proteins for 1 h and a solution of 10% methanol and 10% acetic acid was used to destain them for 1 h. Molecular weight markers (Precision Plus Protein™ 161–0363 All Blue Unstained Protein Standards, Bio-Rad, Mississauga, ON, Canada) were used to estimate the molecular weight. Images of the gels were captured using the ChemiDoc™ MP Imaging System (ChemiDoc MP, Bio-Rad, Mississauga, ON, Canada).

2.6. Particle size distribution

Particle size distribution of IEP and UFDF concentrates was obtained by laser light scattering using a Malvern Mastersizer 3000 instrument (Malvern Panalytical, Malvern, UK) following the protocol of Boukil et al. (2022) with slight modifications. IEP and UFDF suspensions (10% *w/V*) were prepared, and the pH was adjusted to 7 and 9 using 1 M NaOH or 1 M HCl. Suspensions were then centrifuged at 15,000 ×*g* for 15 min at 20 °C to remove insoluble aggregates (Avanti® JE Centrifuge, Beckman Coulter, Inc., CA, USA). The resulting supernatants were then added to the Mastersizer 3000 Hydro SV dispersion unit (Malvern Panalytical, Malvern, UK) until an obscuration of 5% was reached. The refraction index of the particle and dispersant were set at 1.48 and 1.33, respectively. The particle size distribution was expressed as volume density (%). Mealworm protein concentrate at pH 4 was not analysed since this pH value induced protein precipitation resulting in a protein concentration too low in the IEP supernatant recovered after centrifugation to be analysed for particle size distribution.

2.7. Surface hydrophobicity

Surface hydrophobicity was measured according to the protocols of Azagoh et al. (2016) and Boukil et al. (2022). Briefly, IEP and UFDF concentrates were used to prepare a series of solutions with protein concentrations ranging from 0.01% to 0.05% (*w/V*) in 2 mM phosphate buffer at pH 7. Relative fluorescence units (RFU) of the samples with ($RFU_{protein+ANS}$) or without ($RFU_{protein}$) the addition of 8-anilino-1-naphthalene sulfonate (ANS) (8 mM ANS in 0.1 M phosphate buffer at pH 7) were measured using the modular multimode microplate reader BioTek Synergy H1 (Agilent Technologies, Santa Clara, CA, USA). The fluorescence intensity of each protein solution series was measured using an excitation wavelength of 380 nm and an emission wavelength of 460 nm. The extrinsic fluorescence of the samples (RFU_{sample}) was determined by subtracting the intrinsic fluorescence of the proteins ($RFU_{protein}$) and the fluorescence of the phosphate buffer (RFU_{blank}) from the measured fluorescence of the sample ($RFU_{protein+ANS}$), according to Eq. (3):

$$RFU_{sample} = RFU_{protein+ANS} - RFU_{protein} - RFU_{blank} \quad (3)$$

The surface hydrophobicity index (H_0) was determined by calculating the slope of the linear regression analysis of fluorescence intensity as a function of the protein concentration.

2.8. Differential scanning calorimetry (DSC)

The thermal stability of IEP and UFDF concentrates was determined according to the methodology of Queiroz, Regnard, et al. (2021) using a

DSC 250 (TA Instruments, New Castle, DE, USA), equipped with a Refrigerated Cooling System 90. Distilled water (melting point = 0 °C at 1 atm; DHm = 334 J g^{-1}) and indium (melting point = 156.5 °C; DHm = 28.5 J g^{-1}) were used for calibration. Empty hermetically sealed aluminium pans (20 μL volume) were used as references. Nitrogen gas with a flow rate of 50 mL/min was used as the carrier gas. Five to 10 mg of sample was weighed into the aluminium pans, in duplicates. First, the samples were cooled to 0 °C and then scanned from 10 °C to 250 °C at a heating rate of 5 °C/min. The thermograms obtained (heat flow (W/g) as a function of the temperature (°C)) present characteristic peaks, which can be associated with glass transition, thermal unfolding, and solid-melting. Data interpretation was made using TA instruments TRIOS software® (New Castle, DE, USA). Glass transitions were determined from the mid-point of the shift in the curve, while thermal unfolding and solid-melting were determined using the enthalpy and peak maximum.

2.9. Fourier transform infrared spectroscopy (FTIR)

FTIR spectra of *T. molitor* protein concentrates were recorded using a Perkin-Elmer Spectrum 100 spectrometer (Waltham, MA, USA), based on a Universal Attenuated Total Reflectance sensor 125 (UATR-FTIR). As described by Queiroz, Regnard, et al. (2021), the FTIR spectra of the samples were collected over a range of 4000 to 400 cm^{-1} in transmission mode. All spectra were plotted as absorbance (a.u) as a function of wavenumber (cm^{-1}).

2.10. Techno-functional properties

2.10.1. Protein solubility

Protein solubility was determined using the methodology of Morr et al. (1985) with some modifications. Suspensions of IEP and UFDF concentrates (1% *w/V* protein content) were prepared, and the pH of each suspension was adjusted in the range of 2 to 10 using 1 M NaOH or 1 M HCl. The solutions were centrifuged at 20,000 ×*g* for 30 min at 20 °C (Avanti® JE Centrifuge, Beckman Coulter, Inc., CA, USA) and the supernatants were filtered through Whatman® Grade 1 filter paper. The filtrates were freeze-dried (pressure of 27 Pa and plate temperature of 20 °C) (REEP VirTis, SP Scientific, Warminster, PA, USA), and the dried extracts were analysed for their protein content using the Dumas method (Elementar rapid Micro N cube, Langenselbold, Germany) with a nitrogen-to-protein conversion factor of 6.25. The protein solubility was calculated using Eq. (4):

$$Solubility\ (\%) = \frac{protein\ content\ in\ supernatant}{protein\ content\ in\ sample} \times 100 \quad (4)$$

2.10.2. Foaming properties

The foaming capacity (FC) and foam stability (FS) were determined as described by Zielińska et al. (2018) with slight modifications. Protein solutions were prepared by dispersing IEP or UFDF (3% *w/V* protein content) in deionised water, where the pH was adjusted to 4, 7 or 9 with 1 M NaOH or 1 M HCl. The suspensions were then whipped using a hand mixer (KitchenAid, KHM512IB, Benton Charter Township, MI, USA) at maximum speed (1130 rpm) for 4 min and immediately transferred into a graduated cylinder. The total volume of foam was read at time 0 (V_0), and every 15 min for 45 min (V_t). The volume of liquid in the cylinder was also noted (V_{liq}). Foaming capacity and foam stability were calculated using Eqs. (5) and (6), respectively:

$$FC\ (\%) = \frac{V_0 - Vliq}{Vliq} \times 100 \quad (5)$$

$$FS\ (\%) = \frac{V_t - Vliq}{V_0 - Vliq} \times 100 \quad (6)$$

2.10.3. Gelling properties

The least gelling concentration (LGC) of IEP and UFDF concentrates was determined according to the method of Aydemir and Yemenicioglu (2013) with some modifications. Suspensions of IEP and UFDF (12.5, 10, 7.5, 5 and 2.5% *w/V* protein content) were prepared in 0.25 M NaCl, adjusted to pH 4, 7 and 9 with 1 M NaOH or 1 M HCl and heated at 85 °C in a thermoregulated water bath for 1 h. The samples were rapidly cooled by immersing in cold water and then kept at 4 °C for 2 h. To determine if the suspensions had formed a gel, the tubes were inverted at 20 °C. A firm gel was deemed to have formed when the suspensions did not flow upon tube inversion. A weak gel was deemed to have formed when a portion of the suspensions remained at the top of the tube and another portion flowed out upon tube inversion. The LGC was estimated as the critical concentration below which no firm gel was formed.

2.10.4. Emulsifying properties

2.10.4.1. Emulsion preparation. Emulsions containing 0.8% *w/V* protein and 5% *w/V* rapeseed oil were prepared according to the protocol of Queiroz, Casanova, et al. (2021). First, protein suspensions were prepared by dispersing IEP or UFDF concentrates (1% *w/V* protein content) in one of 25 mM citrate buffer (pH 4), 50 mM Tris HCl buffer (pH 7), or 25 mM carbonate-bicarbonate buffer (pH 9). Next, the 1% protein suspensions (continuous phase) were homogenised with rapeseed oil (dispersed phase) using an Ultra-Turrax® (T18, IKA corporation, Germany) for 2 min at 14,000 rpm to produce the emulsions (ratio continuous/dispersed phase = 95/5). Sodium azide (0.05% *w/V*) was added to prevent microbial growth. Finally, the emulsions were stored protected from the light at room temperature (20 °C).

2.10.4.2. Physical stability. To assess the physical stability of the emulsions, a Turbiscan Tower (Formulaction®, Toulouse, France) was used. The technology is based on the principle of static multiple light scattering by illuminating the emulsions with an infrared light source (λ = 880 nm) and collecting the backscattered (BS) and transmitted (T) signals with two sensors. The stability criteria were based on the Turbiscan stability index (TSI), a number calculated at time *t* by summing all temporal and spatial variations in a considered zone (Eq. (7)):

$$TSI_{(t)} = \frac{1}{N_h} \sum_{t_i=1}^{t_{max}} \sum_{z_i=z_{min}}^{z_{max}} |BST\ (t_i, z_i) - BST\ (t_{i-1}, z_i)\,| \quad (7)$$

where t_{max} is the measurement point corresponding to the time *t* at which the *TSI* is calculated, z_{min} and z_{max} are the lower and upper selected height limits, respectively, $N_h = (z_{max} - z_{\min})/\Delta h$ is the number of height positions in the selected zone of the scan, and *BST* is the considered signal (BS if $T < 0.2\%$, and as T otherwise). A TSI value of <3 is considered a reference value for a stable system. Above this value, destabilisation has already started and coalescence, clarification, flocculation or creaming can be observed (Formulaction, 2022). Therefore, a lower TSI indicates a more stable sample.

Following the protocol of Queiroz, Casanova, et al. (2021) with slight modifications, the samples were analysed for 24 h to determine their stability over time. A total of 31 scans were performed during the first hour (0.5 scan per min), 15 scans were performed between 1 and 3.5 h (1 scan every 10 min), and 41 scans were performed until the end of the analysis (1 scan every 30 min). The number of scans was more frequent in the first few hours to observe the onset of emulsion destabilisation.

2.10.4.3. Emulsion droplet size. The droplet size of the emulsions was determined using a laser diffraction method, measured by a Mastersizer 2000 (Malvern Panalytical, Malvern, UK) at T_0 and after 24 h (T_{24}). Following the protocol of Queiroz, Casanova, et al. (2021), emulsion droplets were added into the dispersion unit filled with distilled water and stirred at 3000 rpm, reaching an obscuration of about 12%. The refractive indices of rapeseed oil (1.47) and water (1.33) were used for particles and dispersants, respectively. Results were measured based on

the surface area moment mean diameter (D(3,2)), using Eq. (8):

$$D(3,2) = \frac{\sum n_i d_i^3}{\sum n_i d_i^2} \quad (8)$$

Where n corresponds to the number of droplets with measured diameter, d is the diameter of the droplet, and i represents the size class of the droplets.

2.10.4.4. Flow behaviour. According to the protocol of Kumar et al. (2022), with slight modifications, a Discovery HR-2 rheometer (TA Instruments, New Castle, DE, USA) equipped with a concentric cylinder was employed to characterise the flow behaviour of fresh IEP and UFDF emulsions (T_0) at 22 °C. A 20 mL volume of sample was deposed and analysed for viscosity at a shear rate ranging from 0.01 to 100 s^{-1}. Measurements were performed in duplicate.

2.10.4.5. Confocal laser scanning microscopy. Confocal laser scanning microscopy (CLSM) was performed to explore the microstructure of the emulsions following the protocol of Altay et al. (2023), with few modifications. Briefly, nile red 0.01% (*w/V*) and FCF fast green 0.001% (*w/V*) (Sigma-Aldrich Denmark A/S, Søborg, Denmark) solutions were used to dye the lipid phase and the proteins, respectively. The excitation wavelength for Nile red was 561 nm, and the scanning range of emission wavelength was 600/50 nm. FCF fast green was excited at 640 nm, and the emission wavelength was 700/75 nm. Emulsions were imaged using a 40× lens (Apo LWD water 40× NA 1.15, Nikon, Tokyo, Japan) on a spinning disc confocal microscope, which was composed of an inverted microscope (Nikon Ti2) equipped with a laser source (405/488/561/640 nm), a confocal spinning disc module (Yokogawa CSU-W1, 50 mm pinholes), two single band emission filters (600/50 and 700/75 nm) and a sCMOS camera (Photometrics Prime95B, 11 μm pixel size).

2.11. Statistical analysis

Statistical analysis was carried out using RStudio 4.2.1 software (PBC, Boston, MA, USA). Composition and structural analysis data were subjected to one-way analysis of variance (ANOVA). Solubility and techno-functional properties data were subjected to a two-way ANOVA. Differences between means of the samples were determined using the Tukey test and *p*-values <0.05 were considered statistically significant. All experiments and analyses were performed in triplicate.

3. Results

3.1. Proximate composition, mineral distribution and surface hydrophobicity

The proximate composition of TMM on a dry basis was 42.03 ± 5.66% protein, 32.69 ± 3.10% lipid, 3.60 ± 0.42% ash, 4.80 ± 0.59% chitin, and 1.78 ± 0.84% soluble sugar. Table 1 presents the proximate compositions of the IEP, UFDF, SIEP and PUFDF fractions. The total solids contents were similar for UFDF, IEP and SIEP (ranging from 98.89 to 99.72%) ($p > 0.05$) but lower for PUFDF (95.44%) ($p < 0.05$). The protein content was higher in IEP (80.08%) compared to UFDF (72.20%) ($p < 0.05$) whereas it was much lower but similar for SIEP and PUFDF (40.57 and 37.48%, respectively). The lipid content, not determined in PUFDF due to an insufficient amount of sample, was similar for IEP and UFDF (9.09 and 7.29%, respectively) ($p > 0.05$) and lower for SIEP ($p < 0.05$). In addition, the ash content was lower in the protein fraction generated by IEP compared to UFDF (1.91 and 3.82%, respectively) ($p < 0.05$) but drastically increased in SIEP and PUFDF (36.43 and 45.64%, respectively). The soluble sugar content was significantly higher in UFDF (8.22%) compared to IEP (1.43%) ($p < 0.05$) and similar in both PUFDF and SIEP ($p > 0.05$). Finally, both protein extraction yield and protein process yield were higher for IEP compared to UFDF (27.79 *vs* 21.25% and 71.40 *vs* 64.98%, respectively) ($p < 0.05$).

Table 1
Proximate composition (*w/w*-dry basis) of *T. molitor* fractions (IEP, UFDF, SIEP and PUFDF) as well as protein yields, mineral content, and surface hydrophobicity of IEP and UFDF concentrates.

		UFDF	IEP	PUFDF	SIEP
Total solids (%)		99.72 ± 0.26[a]	99.55 ± 0.69[a]	95.44 ± 0.24[b]	98.89 ± 0.17[a]
Protein (%)		72.20 ± 1.09[a]	80.08 ± 2.96[b]	37.48 ± 0.58[c]	40.57 ± 5.61[c]
Lipid (%)		7.29 ± 0.25[a]	9.09 ± 1.42[a]	–	1.22 ± 0.23[b]
Ash (%)		3.82 ± 0.10[a]	1.91 ± 0.09[b]	45.64 ± 0.49[c]	36.43 ± 0.82[d]
Soluble sugars (%)		8.22 ± 0.12[a]	1.43 ± 0.47[b]	7.77 ± 0.23[a]	6.60 ± 1.63[a]
Protein extraction yield (%)		21.25 ± 3.31[a]	27.79 ± 2.88[b]	–	–
Protein process yield (%)		64.98 ± 3.18[a]	71.40 ± 3.26[b]	–	–
Macrominerals (%)	Na	72.1[a]	88.8[b]	–	–
	Mg	1.4[a]	0.6[b]	–	–
	K	24.4[a]	7.6[b]	–	–
	Ca	1.1[a]	0.4[b]	–	–
Microminerals (%)	Cr	<LOQ	<LOQ	–	–
	Fe	0.2[a]	0.3[b]	–	–
	Mn	<LOQ	<LOQ	–	–
	Co	<LOQ	<LOQ	–	–
	Ni	<LOQ	<LOQ	–	–
	Cu	0.2[a]	1.5[b]	–	–
	Zn	0.4[a]	0.8[b]	–	–
	As	<LOQ	<LOQ	–	–
	Se	<LOQ	<LOQ	–	–
	Sr	<LOQ	<LOQ	–	–
Heavy metals (%)	Cd	<LOQ	<LOQ	–	–
	Hg	<LOQ	<LOQ	–	–
	Pb	<LOQ	<LOQ	–	–
	U	<LOQ	<LOQ	–	–
Total minerals (%)		100	100	–	–
H_0 (a.u)		493.50 ± 43.68[a]	106.78 ± 60.36[b]	–	–

[a,b] Values with a different superscript in the same row are significantly different ($p < 0.05$). LOQ: limit of quantification.

Table 1 also presents the mineral distribution in IEP and UFDF. The most abundant mineral in both IEP and UFDF concentrates was Na (88.8 and 72.2%, respectively), followed by K (7.6 and 24.5%, respectively). The third most abundant mineral was Cu in IEP (1.5%) and Mg in UFDF (1.5%). The contents of Na, Fe, Cu and Zn were significantly higher in IEP than in UFDF ($p < 0.05$) but the contents of Mg, K and Ca were significantly higher in UFDF ($p < 0.05$). The levels of the toxic heavy metals Cd and Pb were low in both concentrates and not of concern for food safety. Finally, the H_0 of UFDF concentrate (493.50) was significantly higher than for IEP concentrate (106.78) ($p < 0.05$) (Table 1).

3.2. Protein structure

3.2.1. Protein profile

Fig. 1A and B show the SDS-PAGE protein profiles of IEP, UFDF, SIEP and PUFDF. Under non-reducing conditions, similar protein profiles were observed for IEP and UFDF with major bands of molecular weight (MW) close to 125, 75, 50, 25 and 18 kDa. A band above 250 kDa (in the gel well) as well as an intense and large band between 10 and 15 kDa were also noted. Under non-reducing conditions, some differences were observed between the IEP and UFDF profiles since a band between 37 and 50 kDa and another band between 15 and 20 kDa were only detected for IEP. Under reducing conditions, the protein profiles of IEP and UFDF were also similar. Indeed, two major bands were detected at 125 and 75 kDa. Several additional bands were noted, including two with MW between 37 and 50 kDa, two with MW between 25 and 37 kDa, two with MW between 15 and 20 kDa, and a large and intense band with

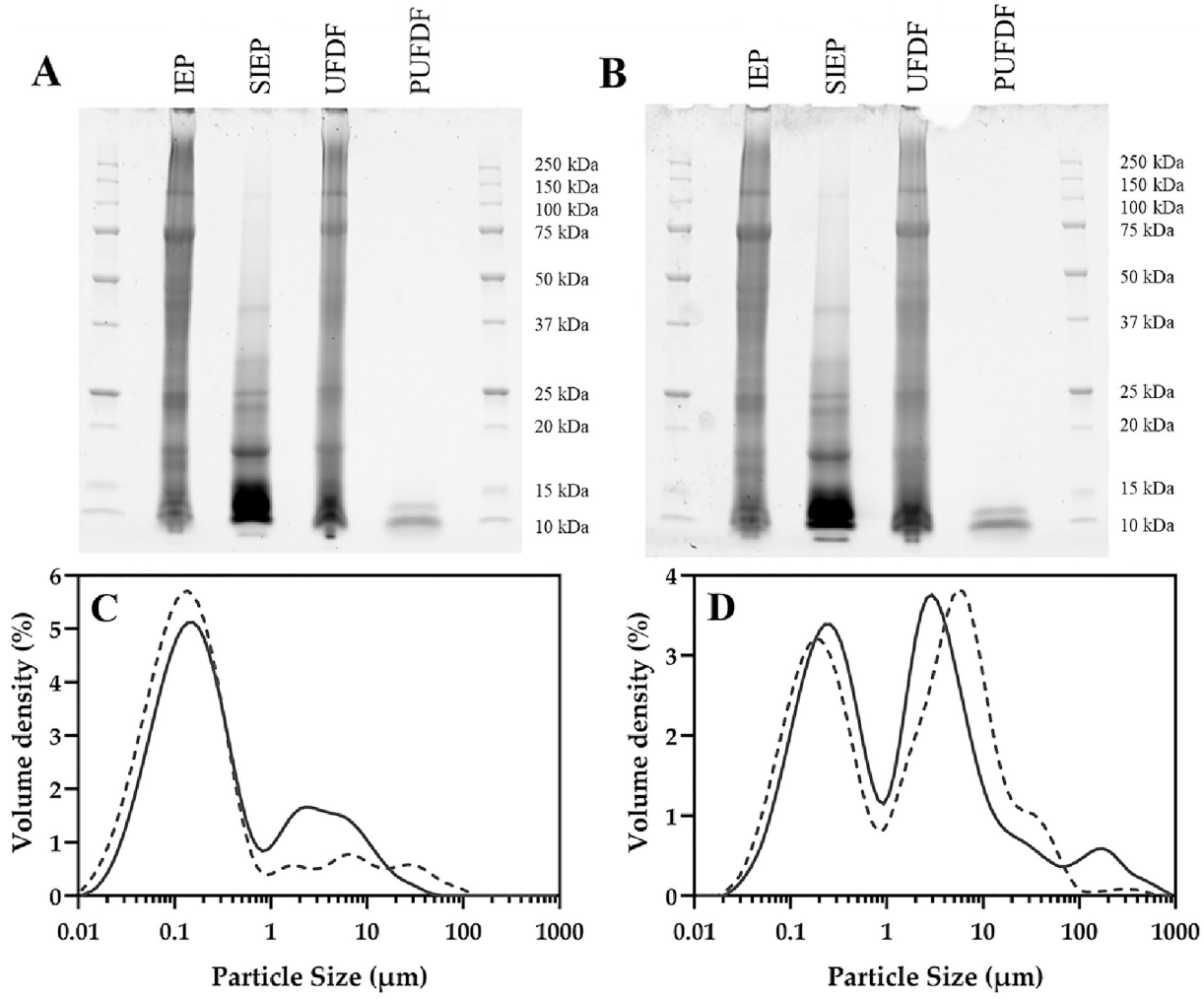

Fig. 1. Non-reducing (A) and reducing (B) SDS-PAGE of concentrates (IEP and UFDF), supernatant from isoelectric precipitation (SIEP) and permeate recovered after ultrafiltration-diafiltration (PUFDF), as well as particle size distribution of IEP (solid line) and UFDF (dotted line) at pH 7 (C) and 9 (D).

MW below 15 kDa. A decrease in band intensity close to 250 kDa and the appearance of bands in the 25 to 50 kDa region in IEP and UFDF profiles were observed only under reducing conditions. Contrary to concentrates, major differences were observed between SIEP and PUFDF. More specifically, several bands close to 125, 40, 25 and 18 kDa were observed in the SIEP profile, including a very large and intense band between 10 and 15 kDa whereas only two bands below 12 kDa appeared in the PUFDF profile.

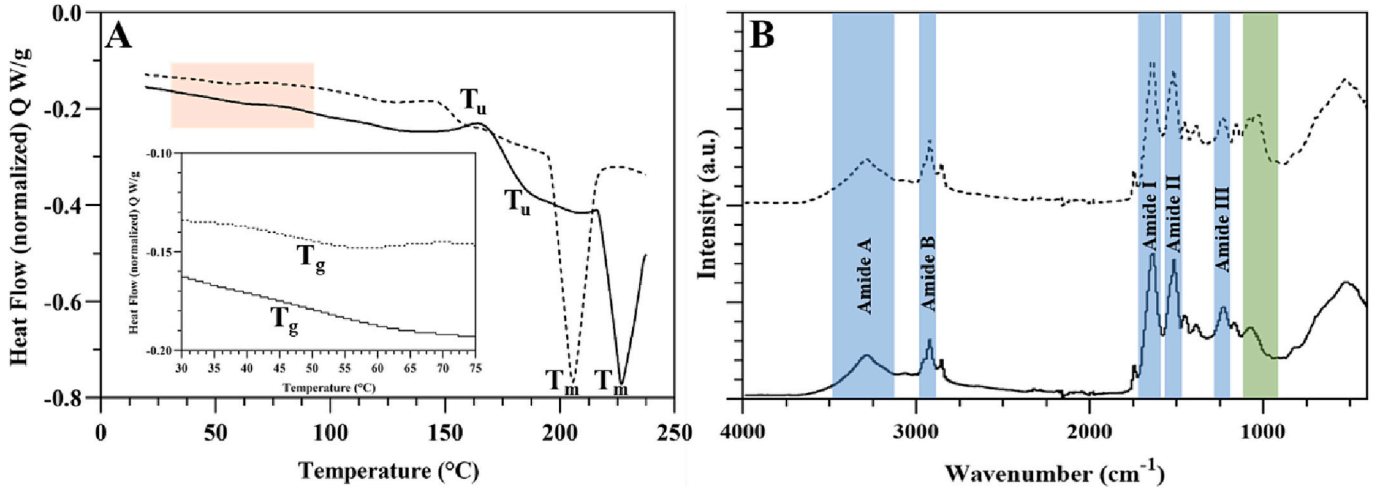

Fig. 2. DSC thermograms (A) and FTIR spectra (B) of IEP (solid line) and UFDF (dotted line).

3.2.2. Particle size

Fig. 1C and D present the particle size distribution for IEP and UFDF at pH 7 and 9. At pH 7, two different particle-size populations were obtained for both concentrates, with a main population at 0.15 μm and a second smaller but large population consisting of particles ranging from 1 to 60 μm for UFDF and from 1 to 100 μm for IEP. This second population was more intense in IEP compared to UFDF (1.5 *vs* 0.8%, respectively). At pH 9, the results showed a bimodal distribution (0.3 and 5 μm) for both protein concentrates. A third smaller population with particle size distribution close to 200 μm was observed only for the IEP sample.

3.2.3. Thermal stability

The DSC thermograms for IEP and UFDF with their respective T_g, T_u, and T_m values, corresponding to glass transition, thermal unfolding, and solid-melting, are presented in Fig. 2A. The glass transition was observed as a shift in the curve at 46.10 °C ± 4.16 °C for IEP and 49.17 °C ± 0.54 °C for UFDF (highlighted in orange). An endothermic peak, resulting from the thermal unfolding of the proteins, was observed at 181.44 °C ± 2.19 °C and 161.32 °C ± 6.38 °C for IEP and UFDF, respectively. The denaturation enthalpy was 1.81 for IEP and 1.06 J g^{-1} for UFDF. An endothermic peak was also observed, corresponding to the melting point at 221.76 °C ± 5.50 °C for IEP (with an enthalpy of 36.29 J g^{-1}) and 211.70 °C ± 8.62 °C for UFDF (with an enthalpy of 43.98 J g^{-1}).

3.2.4. FTIR spectra

Fig. 2B shows the FTIR spectra of IEP and UFDF. Five regions corresponding to the amide groups (highlighted in blue) can be identified on the FTIR spectra due to the presence of peptide bonds between amino acids. Overall, the FTIR spectra were similar for IEP and UFDF. For both concentrates, the amide A group (N—H stretching bonds) was detected around 3285 cm^{-1}; the amide B group (C—H stretching bonds) around 2924 cm^{-1}; the amide I group (C═O stretching bonds) around 1640 cm^{-1}; the amide II group (C—N stretching bonds, N—H bending bonds) around 1514 cm^{-1}; and finally, the amide III group (C—N stretching bonds, N—H bending bonds) around 1230 cm^{-1}. However, a difference was noted in the region close to 1027 cm^{-1} (highlighted in green) with the presence of a peak with a higher intensity for UFDF.

3.3. Techno-functional properties

3.3.1. Protein solubility

Fig. 3A shows the protein solubility of IEP and UFDF from pH 2 to 10. For both concentrates, a typical U-shaped curve was obtained with a minimal protein solubility at pH 4 (2.69 and 18.00%, respectively) which increased when the pH values were far from this pH value. Overall, proteins from the UFDF sample were more soluble than those from IEP. More specifically, the solubility of UFDF increased rapidly between pH 4 and 6 (from 18.00 to 85.37%) and then reached a maximum value of 86% between pH 6 and 10. Contrary to UFDF, the solubility of IEP increased more gradually and reached a maximum of 86% at pH 10.

3.3.2. Foaming properties

The FC results for IEP and UFDF at pH 4, 7 and 9 are shown in Fig. 3B. Due to large standard deviations, no differences were obtained between the samples ($p > 0.05$). However, the FC of UFDF was generally higher compared to IEP, mainly at pH 4 (8.92 *vs* 0.00% for UFDF and IEP) and 7 (14.76 *vs* 2.63% for UFDF and IEP). Moreover, for both concentrates, the FC was positively correlated with pH. Finally, the foam was observed to be unstable over time since the FS values were null (data not shown).

3.3.3. Gelling properties

Table S1 (supplementary material) summarises the gelling properties of IEP and UFDF at different protein concentrations (12.5, 10, 7.5, 5 and 2.5% *w/V*) and pH values (4, 7 and 9). Each of the three samples (IEP1, 2 and 3 and UFDF1, 2 and 3) from the same triplicate (IEP and UFDF) was studied separately. The results showed that a minimum protein concentration of 10% was required to induce the formation of a firm gel for most of the samples. The LGC of samples IEP3 pH 7, UFDF2 pH 4, and UFDF3 (pH 4, 7 and 9) was 12.5%. At pH 4, IEP has a LGC above 12.5%. The results also showed that at pH 7 and 9, and for protein concentrations of 5% or lower, UFDF did not form a gel, contrary to IEP (except for IEP1 at pH 9).

3.3.4. Emulsifying properties

3.3.4.1. Physical stability. The results presented in Fig. S2 (supplementary material) showed that both emulsions at pH 4 reached a TSI equal to 3 in <2 min. At pH 7, IEP and UFDF emulsions reached this value in 6 and 28 min, respectively. At pH 9, a TSI of 3 was reached in 15 and 34 min for IEP and UFDF emulsions, respectively. The ΔBS profiles of the emulsions as a function of the height of the sample can be found in Fig. S3 (supplementary material). IEP and UFDF emulsions at pH 7 and 9 showed a creaming phenomenon, where the ΔBS signal decreased at the bottom and increased at the top because of coalescence and migration of droplets to the top. The negative ΔBS signal at the top in IEP emulsions at pH 7 and 9 represents formation of a fat layer whereas the positive ΔBS signal at the bottom represents a sedimentation phenomenon. The two emulsions at pH 4 showed a more complex destabilisation behaviour with creaming and sedimentation phenomena still being present but appearing more rapidly.

3.3.4.2. Emulsion droplet size. The mean droplet surface size of IEP and UFDF emulsions at different times (0 min (T_0) and after 24 h (T_{24})) and pH values (4, 7 and 9) are reported in Table 2. First, whether at T_0 or T_{24}, the emulsion droplets were significantly larger at pH 4 compared to pH 7

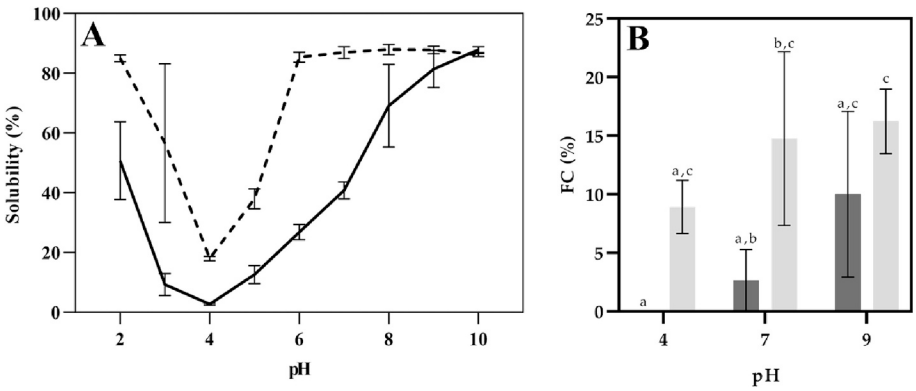

Fig. 3. Protein solubility of IEP (solid line) and UFDF (dotted line) from pH 2–10 (A) and foaming capacity at pH 4, 7 and 9 for IEP (black) and UFDF (grey) (B).

Table 2
Mean droplet surface size (μm) of IEP and UFDF emulsions at different times (T_0 and T_{24}) and at different pH (4, 7 and 9).

Time	Samples	pH 4	pH 7	pH 9
T_0	IEP	20.71 ± 2.14^{a}	2.32 ± 0.10^{c}	2.90 ± 0.86^{c}
	UFDF	17.73 ± 0.70^{b}	0.70 ± 0.10^{c}	1.02 ± 0.06^{c}
T_{24}	IEP	19.52 ± 0.31^{a}	0.71 ± 0.03^{c}	0.42 ± 0.05^{c}
	UFDF	13.23 ± 0.47^{b}	0.28 ± 0.01^{c}	0.33 ± 0.02^{c}

[a,b] Values with a different superscript are significantly different ($p < 0.05$).

and 9 for both samples ($p < 0.05$). Furthermore, the droplet size of UFDF emulsions was consistently smaller than that of IEP emulsions, regardless of pH and time. However, this difference was only significant at pH 4 ($p < 0.05$). Finally, for all samples, the results showed a decrease in droplet size after 24 h.

3.3.4.3. Flow behaviour. The results presented in Fig. S4 (supplementary material) show the viscosity as a function of the shear rate of IEP and UFDF emulsions at different pH values. All emulsions showed a decrease in viscosity with increasing shear, representing non-Newtonian

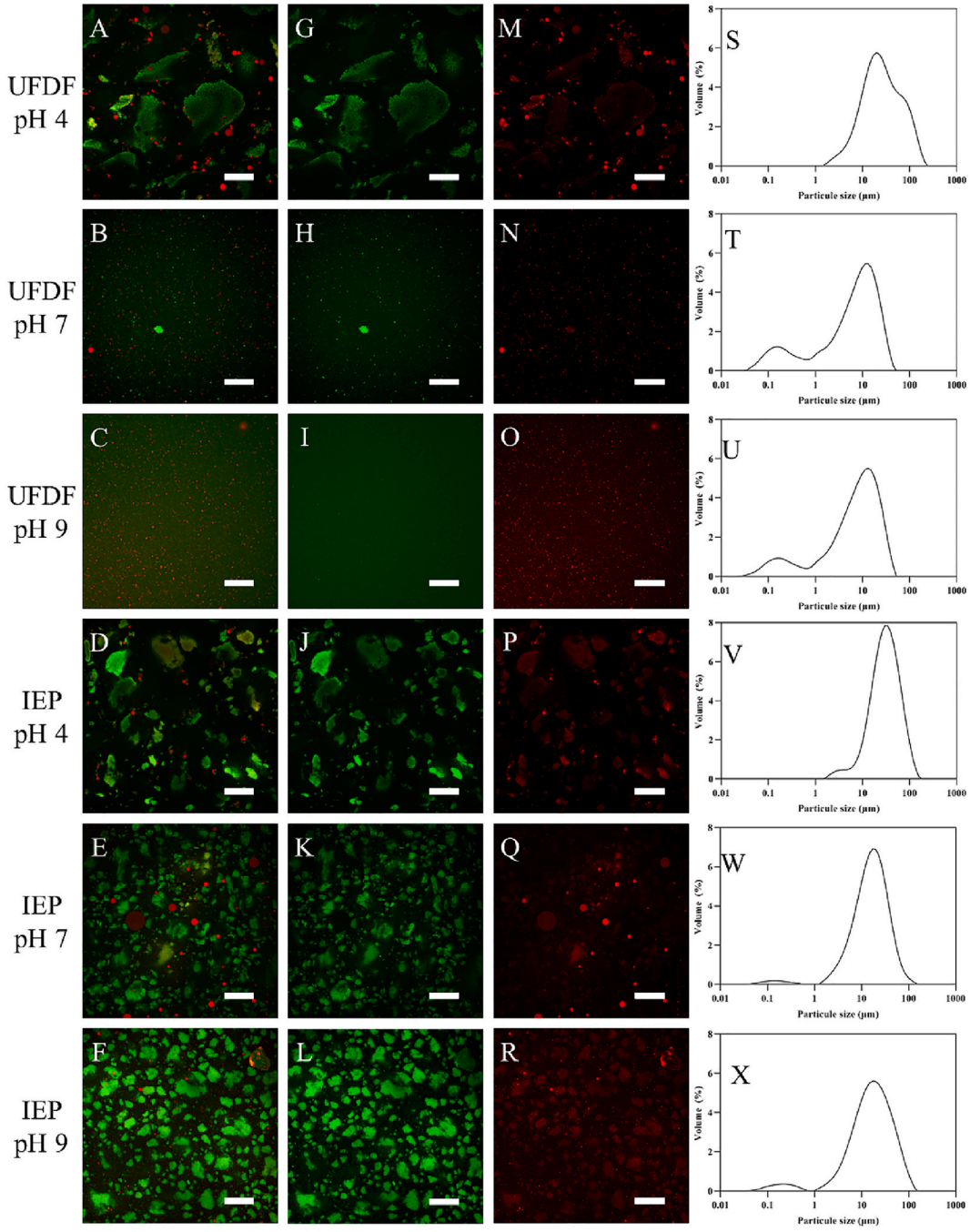

Fig. 4. Confocal laser scanning microscopy (CLSM) images of UFDF (A), (B), (C) and IEP (D), (E), (F) emulsions at pH 4, 7 and 9. CLSM images were realised at 700 nm emission bands for FCF green for UFDF (**G**), (**H**), (**I**) and IEP (**J**), (**K**), (**L**), and at 600 nm emission bands for Nile red for UFDF (**M**), (**N**), (**O**) and IEP (**P**), (**Q**), (**R**) emulsions at pH 4, 7 and 9, respectively. The droplet size distribution of UFDF is shown in (S), (T), (U) and IEP is shown in (V), (W), (X) for emulsions at pH 4, 7 and 9. Green and red colours indicate protein and fat. The void area appears black. The scale bar is 50 μm for all images. (For interpretation of the references to colour in this figure legend, the reader is referred to the web version of this article.)

flow behaviour and, more precisely, the emulsions can be described as shear-thinning fluids.

3.3.4.4. Confocal laser scanning microscopy. Fig. 4 presents the CLSM images and the droplet size distributions (at T_0, *i.e.*, at the time the CLSM images were taken) of UFDF and IEP emulsions at pH 4, 7 and 9. The results showed that UFDF and IEP emulsions at pH 4 (Fig. 4A and D) exhibited the largest protein aggregates. While large fat droplets were found between these aggregates, other smaller lipid droplets appeared to be trapped within the protein aggregates since the signals for both dyes were colocalised. At pH 7 and 9, UFDF emulsions did not show protein aggregates, but proteins and very small fat droplets homogeneously dispersed (Fig. 4B and C). Conversely, at pH 7 and 9, IEP emulsions contained protein aggregates, more numerous but smaller and less spaced than those at pH 4 (Fig. 4E and F). In IEP emulsions, fat was also trapped within the protein aggregates and larger fat droplets were found between these aggregates at pH 7. For the droplet size distribution, shoulder distributions for both samples were visualized at pH 4, with a main population at 35 μm for the IEP emulsion (7.8%) (Fig. 4V), and approximately 22 μm for the UFDF emulsion (5.7%) (Fig. 4S). At pH 7 and 9, the distributions of UFDF emulsions were very similar. Indeed, two different populations were obtained, a main population around 10 μm (5.5%) and a second smaller population at 0.15 μm (1%) (Fig. 4T and U). For IEP emulsions, bimodal distributions can also be observed, with a main population at 20 μm (6.8% at pH 7 and 5.6% at pH 9), and a second smaller population at 0.15 (0.3%) and 0.2 (0.35%) μm for pH 7 and 9, respectively (Fig. 4W and X).

4. Discussion

4.1. Influence of the processing on the proximate composition and mineral distribution

The significantly lower total solids content of PUFDF (95.44%) ($p < 0.05$) compared to the other fractions (Table 1) was related to its high hygroscopicity since PUFDF are mainly composed of water and minerals, especially Na + from the addition of NaOH during the alkaline solubilization step. Consequently, we hypothesized that PUFDF absorb moisture from the ambient atmosphere during total solids content measurement steps (See et al., 2023). This tendency has already been observed in other studies (Gravel et al., 2023). The protein contents of IEP (80.08%) and UFDF (72.20%) were in accordance with previous results on mealworm protein concentrates generated by IEP (Bußler et al., 2016; Laroche et al., 2022; Ravichandran et al., 2019). The higher protein content obtained for IEP compared to UFDF (Table 1) could be related to a concentration effect due to IEP's lower ash and soluble sugars contents. That the protein extraction yield obtained for IEP (27.79%) was lower than those found by Ravichandran et al. (2019) (38.8%) and Laroche et al. (2022) (49.5%) on *T. molitor* is probably explained by differences in initial mealworm meal composition as well as process and parameters applied for the blanching and killing steps. Moreover, no defatting step with solvent was applied in our work, contrary to the studies of Ravichandran et al. (2019) and Laroche et al. (2022). The protein yields of IEP were higher compared to those of UFDF (Table 1). This result is quite surprising since only proteins with an isoelectric point close to 4.5 can be precipitated whereas UFDF, at the molecular weight cut-off tested (30 kDa), should retain all proteins as observed in our previous work (Berthelot et al., 2023). This difference could result in the loss of proteins in UF-retentate that occurred during various stages of the UFDF process (recovery of UFDF concentrate as well as rinsing and cleaning steps due to the dead volumes of the UF system). The higher fat content obtained for IEP and UFDF (9.09 and 7.29%) compared to the value reported by Bußler et al. (2016) (0.4%) for a mealworm protein concentrate generated by IEP is explained by the hexane defatting step used by these authors, which is more effective for removing the lipid fraction than the cold centrifugation used in our work (Zielińska, 2022). However, in our protocol, cold centrifugation was preferred over solvent for removing lipids in order to preserve the native structure of the proteins (Gravel et al., 2021). The lower ash content in IEP (1.91%) compared to UFDF (3.82%) is consistent with the study of Mondor et al. (2009) who also reported a reduction of 32 to 39% in ash content in chickpea protein concentrates produced by IEP compared to UFDF. The addition of HCl and NaOH protein concentrate for protein precipitation at pH 4.5 and concentrate neutralization at pH 7 was intended to enhance the ash concentration. However, as done by Mondor et al. (2009) and in the present work, the washing steps applied to the protein precipitate decreased the mineral content. The process also influenced the soluble sugar content in concentrates which was 6 times higher in UFDF (8.22%) compared to IEP (1.43%) (Table 1). This result could be explained by the retention of several soluble sugars in the UF retentate whereas no sugar precipitation occurred during IEP at pH 4.5. Indeed, Sergius-Ronot et al. (2023) also noticed retention of human milk oligosaccharides by UF membrane with MW cut-off of 50 kDa.

Several authors who have previously studied the mineral composition of mealworms reported that *T. molitor* larvae are particularly rich in K, P, Mg, Na and Fe (Gkinali et al., 2022; Ravzanaadii et al., 2012), which is consistent with our results showing that Na, K, Cu and Mg were the most abundant minerals in IEP and UFDF (Table 1). Overall, the process impacted the distribution of the 6 minerals detected above the limit of quantification (Na, Mg, K, Ca, Fe, Cu, Zn).

4.2. Influence of the processing on the protein profile and structure

The production method had only a minor impact on the protein profiles (Fig. 1A and B) and particle size (Fig. 1C and D) of IEP and UFDF mealworm protein concentrates.

The slight differences in protein profiles observed between the non-reduced and reduced gels for concentrates and SIEP/PUFDF indicated minimal involvement of disulfide bonds in the mealworm protein structure, which could be due to their low cysteine content as found by Ravzanaadii et al. (2012). Contrary to the concentrates, major changes were observed for both SIEP and PUFDF in terms of number of bands and their MW. Indeed, the bands visualized in SIEP indicated that several proteins remained soluble at the isoelectric point of mealworm protein (pH 4.5). Thus, the two bands detected in SIEP with MW around 18 and 25 kDa could potentially originate from *T. molitor* cuticle proteins, including chymotrypsin-like proteinase (24 kDa) (Bußler et al., 2016; Yi et al., 2013). The band with a MW close to 40 kDa could correspond to enzymes or other proteins, *e.g.*, melanisation-inhibiting protein (43 kDa) (Bußler et al., 2016;Gravel et al., 2021; Yi et al., 2013). Finally, the band with a MW of approximately 125 kDa probably corresponds to vitellogenin like proteins (Bußler et al., 2016). Conversely, the two low-intensity bands detected in PUFDF validated the high retention of mealworm proteins by the 50-kDa UF membrane (Berthelot et al., 2023). Moreover, the low MW proteins (<15 kDa), typically observed in previous studies, could be associated with non-protein nitrogen, as suggested previously (Berthelot et al., 2023), and anti-freeze type proteins, such as haemolymph proteins (12 kDa) (Gravel et al., 2021; Yi et al., 2013).

The particle size distribution of concentrate solutions obtained at pH 7 was similar to the results published by Boukil et al. (2022), who extracted proteins from mealworm using IEP. The pH value seemed to modify the particle size distribution of concentrates since an increase from 7 to 9 increased the volume density of the second population. However, due to its large size, this second population likely corresponded to residual lipids rather than proteins.

As mentioned in Table 1, the much lower H_0 value obtained for IEP compared to UFDF was probably due to protein aggregation induced by IEP, as already observed for soybean proteins (Wang et al., 2014). This aggregation could reduce exposure of hydrophobic areas or reduce accessibility of the probe.

Overall, the thermal stability observed for IEP and UFDF was consistent with the study of Queiroz, Regnard, et al. (2021). Indeed, these authors indicated a T_g between 45 and 60 °C, a T_u around 150 °C and a T_m at 200 °C for *Hermetia illucens* larvae protein concentrates. In both curves, the slight exothermic peak observed before T_u could be related to the fat in the samples or other residues (Queiroz, Regnard, et al., 2021). The higher T_u value obtained for IEP (181.44 °C) compared to UFDF (161.32 °C) ($p < 0.05$) could be because the proteins were in a more native state in UFDF compared to IEP and therefore their denaturation temperature was lower.

Finally, the production method seemed to have no impact on the secondary structure of *T. molitor* proteins since the FTIR spectra of both concentrates were similar (Fig. 2B). In addition, the amide I group that was prominent in both spectra correlated directly with the secondary structure of the proteins since this region contained β-sheets, α-helices, and random coil structures (Queiroz, Casanova, et al., 2021). The peak observed around 1027 cm^{-1} with higher intensity for UFDF compared to IEP could be due to the C—O bonds of the carbohydrates present between 1200 and 900 cm^{-1} (Queiroz, Casanova, et al., 2021; Queiroz, Regnard, et al., 2021), which was consistent with the proximate composition of UFDF in terms of higher soluble sugar content compared to IEP.

4.3. Influence of the processing on the techno-functional properties

As expected, the solubility (Fig. 3A) was minimal at the pH corresponding to the IEP of *T. molitor* proteins due to protein-protein interactions (Bußler et al., 2016) and maximal at both acidic and alkaline pH extremes tested since positive or negative charges promote stronger interactions with the solvent (water). As reported in this work and by Boye et al. (2010) on pulses, UFDF protein concentrates showed overall better solubility compared to those produced by IEP, except at pH 9 and 10 where solubility was similar for both methods. Indeed, the protein native state was probably better preserved by UFDF compared to IEP (Rao et al., 2002).

The foaming properties of the protein concentrates were unaffected by pH or the processing method (Fig. 3B). This is consistent with the work of Boye et al. (2010) who reported non-significant differences in foaming capacity between protein concentrates from three pulses produced by IEP and UFDF. In addition, several authors (Gravel et al., 2021; Yi et al., 2013; Zielińska et al., 2018) have reported that the foaming properties of non-defatted *T. molitor* extracts were lower than for defatted extracts, consistent with the low FC values obtained in our concentrates due to their residual lipid contents (7.29 for IEP and 9.9 for UFDF).

The gelling properties of mealworm protein concentrates were similar to those produced by Boye et al. (2010) with the LGC ranging from 8 to 14%. However, in contrast to our results, Boye et al. (2010) showed the impact of the production process since pulse protein concentrates generated by UFDF exhibited better gelling properties compared to those obtained by IEP. This difference could be explained by a matrix effect since our mealworm proteins produced by IEP tend to aggregate and precipitate to form a pellet, even at pH values far from the isoelectric point, which could promote gel formation at the bottom of the tubes.

The emulsion stability was influenced by both the extraction method and the pH (Fig. S2), which was expected since the extraction method and pH also influenced the emulsion droplet size (Table 2). Thus, the very low stability of the emulsions at pH 4 was explained by the significantly larger droplet size at this pH ($p < 0.05$). Moreover, UFDF emulsions tend to have smaller droplet sizes than IEP emulsions, which is consistent with our results showing that UFDF emulsions are more stable over time. Moreover, the decrease in droplet size during the 24-h analysis was probably related to the larger droplets that had coalesced and come to the surface, while the smaller droplets remained in the centre of the beaker where the samples were collected for analysis. Furthermore, neither the processing method nor the pH influenced the viscosity of the emulsions, which all exhibited non-Newtonian shear-thinning behaviour with similar viscosity values. This shear-thinning behaviour might be a result of the deformation and realignment of flocculated droplets along with the shear field (McClements, 2015). In Fig. S4, the IEP emulsion at pH 4 appeared to have the lowest viscosity, which seemed to be inconsistent with the particle size (Table 2) and CLSM (Fig. 4) data showing that the IEP emulsion at pH 4 exhibited protein aggregates. However, being very close to the isoelectric point of mealworm proteins at pH 4, these aggregates quickly sedimented to the bottom of the beaker (faster than the UFDF emulsion at pH 4), which explains why the measured viscosity tended to be lower for the IEP at pH 4. The emulsion microstructures were studied using CLSM (Fig. 4) to further support the results on emulsion stability and droplet size. At pH 4, both samples had large protein aggregates, which was consistent with the low solubility and intense protein aggregation close to the isoelectric point. The presence of these aggregates also explains the lack of stability of UFDF and IEP emulsions obtained at pH 4. According to the particle size distribution results, the average size based on the surface area moment mean diameter of these aggregates was 35 μm for UFDF emulsions and 22 μm for IEP emulsions, which is consistent with what can be observed in the CLSM images. Moreover, at pH 7 and 9, UFDF emulsions did not show any aggregates in the CLSM images indicating that proteins and lipids were well dispersed within the emulsions. This is consistent with previous results (Fig. S2 and Table 2) showing that these were the two most stable emulsions with the smallest droplet size. The droplet size distribution of these two emulsions showed the main population of droplets having <10 μm particle diameter and a second smaller population of around 0.15 μm diameter, which is consistent with the images obtained. In contrast, at pH 7 and 9, the IEP emulsions had a more compact structure of protein aggregates, which explains why they were less stable over time than the UFDF emulsions. The solubility results had already shown that IEP proteins are less soluble and therefore have a greater tendency to aggregate than UFDF proteins. Moreover, in the CLSM images, the aggregates of IEP emulsions appeared smaller at pH 7 and 9 than at pH 4, which was confirmed by the droplet size distribution results showing the main population at approximately 20 μm (*versus* 22 μm at pH 4). Overall, the processing method as well as the pH greatly influenced the emulsifying properties of the two protein concentrates studied.

5. Conclusion

This study showed that the IEP process resulted in a higher protein content (80 *versus* 72%) but lower ash contents (1.91 *versus* 3.82%) and soluble sugar content (1.43 *versus* 8.22%) than UFDF. In addition, the protein extraction and process yields were higher for IEP compared to UFDF. However, only minor impacts were noticed on the mealworm protein structure, except for a higher denaturation temperature for IEP (161.32 *versus* 181.44 °C) and higher surface hydrophobicity for UFDF (493.5 *versus* 106.78 a.u). Finally, the production method did not influence the foaming and gelling properties of the protein concentrates, but UFDF provided better protein solubility (87 *versus* 41%) and emulsifying properties. For example, UFDF emulsions were more stable than IEP emulsions at pH 9 (34 *versus* 15 min) and at pH 7 (28 *versus* 6 min). Consequently, UFDF could be considered most interesting of these two technologies for the use of mealworm protein concentrates in different formulations whereas IEP was more efficient at generating a concentrate with higher protein content. Further studies could be initiated for the optimization of technical parameters during IEP and UFDF steps to improve the protein content of concentrates. In addition, for future developments, both concentrates could be used as raw materials in digestibility studies, for the development of food formulations and to evaluate their properties (texture, viscosity, stability, *etc.*). Moreover, it would be relevant to further explore the nutritional values of the concentrates by studying, for instance, the essential amino acid profile and

the biological value (*e.g.* PDCAAS). Furthermore, economic, environmental (*e.g.* life cycle assessment) and social (*e.g.* consumer acceptance) indicators supporting the commercial-scale production of mealworm protein concentrates should be evaluated. Finally, it will be crucial to validate the microbiological safety of mealworm concentrates prior to their use as ingredients in the food sector.

CRediT authorship contribution statement

Gwenn Pinel: Writing – review & editing, Writing – original draft, Formal analysis, Data curation, Conceptualization. **Ugo Berthelot:** Writing – review & editing, Supervision, Conceptualization. **Lucas Sales Queiroz:** Writing – review & editing. **Livia De Almeida Santiago:** Writing – review & editing. **Naaman Francisco Nogueira Silva:** Writing – review & editing. **Heidi Olander Petersen:** Writing – review & editing, Formal analysis. **Jens J. Sloth:** Writing – review & editing. **Ipek Altay:** Writing – review & editing, Formal analysis. **Rodolphe Marie:** Writing – review & editing. **Aberham Hailu Feyissa:** Writing – review & editing. **Federico Casanova:** Writing – review & editing, Supervision, Resources, Conceptualization. **Alain Doyen:** Writing – review & editing, Supervision, Resources, Conceptualization.

Declaration of competing interest

The authors declare that they have no known competing financial interests or personal relationships that could have appeared to influence the work reported in this paper.

Data availability

Data will be made available on request.

Acknowledgements

This research was funded by the Innov'Action research program of the MAPAQ (Ministry of Agriculture, Fisheries and Food, Government of Québec (IA222729)). The authors would like to thank Groupe Neoxis Inc. (Saint-Flavien, Quebec, Canada) for kindly providing *T. molitor* larvae. The authors also thank Diane Gagnon, Mélanie Martineau, Véronique Perreault, and Pascal Lavoie of the department of Food Sciences of Université Laval for the technical assistance with experiments.

Appendix A. Supplementary data

Supplementary data to this article can be found online at https://doi.org/10.1016/j.foodchem.2024.139177.

References

Altay, I., Queiroz, L. S., Silva, N. F. N., Feyissa, A. H., Casanova, F., Sloth, J. J., & Mohammadifar, M. A. (2023). Effect of moderate electric fields on the physical and chemical characteristics of cheese emulsions. *Gels, 9*(9), 747. https://doi.org/10.3390/gels9090747

Aydemir, L. Y., & Yemenicioglu, A. (2013). Potential of Turkish Kabuli type chickpea and green and red lentil cultivars as source of soy and animal origin functional protein alternatives. *Food Science and Technology, 50*, 686–694. https://doi.org/10.1016/j.lwt.2012.07.023

Azagoh, C., Ducept, F., Garcia, R., Rakotozafy, L., Cuvelier, M. E., Keller, S., … Mezdour, S. (2016). Extraction and physicochemical characterization of *Tenebrio molitor* proteins. *Food Research International, 88*, 24–31. https://doi.org/10.1016/j.foodres.2016.06.010

Berthelot, U., Ricci Piché, S., Brisson, G., & Doyen, A. (2023). *Exploring the use of ultrafiltration-diafiltration for the concentration and purification of mealworm proteins.* Manuscript submitted for publication.

Boukil, A., Marciniak, A., Mezdour, S., Pouliot, Y., & Doyen, A. (2022). Effect of high hydrostatic pressure intensity on structural modifications in mealworm (*Tenebrio molitor*) proteins. *Foods, 11*(7), 956. https://doi.org/10.3390/foods11070956

Boye, J., Aksay, S., Roufik, S., Ribéreau, S., Mondor, M., Farnworth, E., & Rajamohamed, S. H. (2010). Comparison of the functional properties of pea, chickpea and lentil protein concentrates processed using ultrafiltration and isoelectric precipitation techniques. *Food Research International, 43*, 537–546. https://doi.org/10.1016/j.foodres.2009.07.021

Bußler, S., Rumpold, B. A., Jander, E., Rawel, H. M., & Schluter, O. K. (2016). Recovery and techno-functionality of flours and proteins from two edible insect species: Meal worm (*Tenebrio molitor*) and black soldier fly (*Hermetia illucens*) larvae. *Heliyon, 2*(12). https://doi.org/10.1016/j.heliyon.2016.e00218

Dill, K. A., & Shortle, D. (1991). Denatured states of proteins. *Annual Review of Biochemistry, 60*(1), 795–825. https://doi.org/10.1146/annurev.bi.60.070191.004051

Dobermann, D., Swift, J. A., & Field, L. M. (2017). Opportunities and hurdles of edible insects for food and feed. *Nutrition Bulletin, 42*(4), 293–308.

Doran, P. M. (2012). *Bioprocess engineering principles* (2nd ed.). Academic Press.

Formulaction. (2022). Turbiscan stability index. https://formulaction.com/en/knowledge-center/turbiscan-stability-index.

Giannoccaro, E., Wang, Y. J., & Chen, P. (2006). Effects of solvent, temperature, time, solvent to-sample ratio, sample size, and defatting on the extraction of soluble sugars in soybean. *Food Chemistry and Toxicology, 71*(1), 59–64. https://doi.org/10.1111/j.1365-2621.2006.tb12389.x

de Gier, S., & Verhoeckx, K. (2018). Insect (food) allergy and allergens. *Molecular Immunology, 100*, 82–106. https://doi.org/10.1016/j.molimm.2018.03.015

Gkinali, A. A., Matsakidou, A., Vasileiou, E., & Paraskevopoulou, A. (2022). Potentiality of *Tenebrio molitor* larva-based ingredients for the food industry: A review. *Trends in Food Science & Technology, 119*, 495–507.

Gravel, A., & Doyen, A. (2020). The use of edible insect proteins in food: Challenges and issues related to their functional properties. *Innovative Food Science and Emerging Technologies, 59*. https://doi.org/10.1016/j.ifset.2019.102272

Gravel, A., Dubois-Laurin, F., & Doyen, A. (2023). Effects of hexane on protein profile and techno-functional properties of pea protein isolates. *Food Chemistry, 406*, 1–11. https://doi.org/10.1016/j.foodchem.2022.135069

Gravel, A., Marciniak, A., Couture, M., & Doyen, A. (2021). Effects of hexane on protein profile, solubility and foaming properties of defatted proteins extracted from *Tenebrio molitor* larvae. *Molecules, 26*(2). https://doi.org/10.3390/molecules26020351

Henchion, M., Hayes, M., Mullen, A. M., Fenelon, M., & Tiwari, B. (2017). Future protein supply and demand: Strategies and factors influencing a sustainable equilibrium. *Foods, 6*(7). https://doi.org/10.3390/foods6070053

Janssen, R. H., Vincken, J. P., Van Den Broek, L. A., Fogliano, V., & Lakemond, C. M. (2017). Nitrogen-to-protein conversion factors for three edible insects: *Tenebrio molitor*, *Alphitobius diaperinus*, and *Hermetia illucens*. *Journal of Agricultural and Food Chemistry, 65*, 2275–2278. https://doi.org/10.1021/acs.jafc.7b00471

Kumar, S., Queiroz, L. S., Marie, R., Nascimento, L. G. L., Mohammadifar, M. A., de Carvalho, A. F., … Casanova, F. (2022). Gelling properties of black soldier fly (*Hermetia illucens*) larvae protein after ultrasound treatment. *Food Chemistry, 386*, Article 132826. https://doi.org/10.1016/j.foodchem.2022.132826

La Barbera, F., Verneau, F., Amato, M., & Grunert, K. (2018). Understanding Westerners' disgust for the eating of insects: The role of food neophobia and implicit associations. *Food Quality and Preference, 64*, 120–125. https://doi.org/10.1016/j.foodqual.2017.10.002

Laroche, M., Perreault, V., Marciniak, A., Gravel, A., Chamberland, J., & Doyen, A. (2019). Comparison of conventional and sustainable lipid extraction methods for the production of oil and protein isolate from edible insect meal. *Foods, 8*(11). https://doi.org/10.3390/foods8110572

Laroche, M., Perreault, V., Marciniak, A., Mikhaylin, S., & Doyen, A. (2022). Eco-efficiency of mealworm (*Tenebrio molitor*) protein extracts. *Food Science and Technology, 2*, 1077–1085. https://doi.org/10.1021/acsfoodscitech.2c00014

Leni, G., Tedeschi, T., Faccini, A., Pratesi, F., Folli, C., Puxeddu, I., Migliorini, P., Gianotten, N., Jacobs, J., Depraetere, S., Caligiani, A., & Sforza, S. (2020). Shotgun proteomics, in-silico evaluation and immunoblotting assays for allergenicity assessment of lesser mealworm, black soldier fly and their protein hydrolysates. *Scientific Reports, 10*(1). https://doi.org/10.1038/s41598-020-57863-5. Article 1.

Lo, B., Kasapis, S., & Farahnaky, A. (2021). Lupin protein: Isolation and techno-functional properties, a review. *Food Hydrocolloids, 112*. https://doi.org/10.1016/j.foodhyd.2020.106318

McClements, D. J. (2015). *Food emulsions: Principles, practices, and techniques* (3rd ed.). CRC Press.

Mondor, M., Aksay, S., Drolet, H., Roufik, S., Farnworth, E., & Boye, J. (2009). Influence of processing on composition and antinutritional factors of chickpea protein concentrates produced by isoelectric precipitation and ultrafiltration. *Innovative Food Science and Emerging Technologies, 10*, 342–347. https://doi.org/10.1016/j.ifset.2009.01.007

Morr, C. V., German, B., Kinsella, J. E., Regenstein, J. M., Van Buren, J. P., Kilara, A., … Mangino, M. E. (1985). A collaborative study to develop a standardized food protein solubility procedure. *Journal of Food Science, 50*, 1715–1718. https://doi.org/10.1111/j.1365-2621.1985.tb10572.x

Queiroz, L. S., Casanova, F., Feyissa, A. H., Jessen, F., Ajallouеian, F., Perrone, I. T., … Yesiltas, B. (2021). Physical and oxidative stability of low-fat fish oil-in-water emulsions stabilized with Black Soldier Fly (*Hermetia illucens*) larvae protein concentrate. *Foods, 10*(2977). https://doi.org/10.3390/foods10122977

Queiroz, L. S., Regnard, M., Jessen, F., Mohammadifar, M. A., Sloth, J. J., Peterson, H. O., … Casanova, F. (2021). Physico-chemical and colloidal properties of protein extracted from black soldier fly (*Hermetia illucens*) larvae. *International Journal of Biological Macromolecules, 186*, 714–723. https://doi.org/10.1016/j.ijbiomac.2021.07.081

Ranasinghe, M. K., Ballon, A., Lamo-Castellví, S., Ferrando, M., & Güell.. (2023). Ultrafiltration of Black Soldier Fly (*Hermetia illucens*) and mealworm (*Tenebrio*

molitor) protein concentrates to enhance emulsifying and foaming properties. *Membranes, 13*(137). https://doi.org/10.3390/membranes13020137

Rao, A., Shallo, H. E., Ericson, A. P., & Thomas, R. L. (2002). Characterization of soy protein concentrate produced by membrane ultrafiltration. *Journal of Food Science, 67*(4), 1412–1418. https://doi.org/10.1111/j.1365-2621.2002.tb10299.x

Ravichandran, S., Yadav, B. K., & Rawson, A. (2019). Optimization of protein extraction from yellow mealworm larvae. *International Journal of Chemical Studies, 7*(3), 4577–4582.

Ravzanaadii, N., Kim, S. H., Choi, W. H., Hong, S. J., & Kim, N. J. (2012). Nutritional value of mealworm, *Tenebrio molitor* as food source. *International Journal of Industrial Entomology, 25*(1), 93–98. https://doi.org/10.7852/ijie.2012.25.1.093

Rumpold, B. A., & Schlüter, O. K. (2013). Potential and challenges of insects as an innovative source for food and feed production. *Innovative Food Science & Emerging Technologies, 17*, 1–11. https://doi.org/10.1016/j.ifset.2012.11.005

See, X. Y., Dupas-Langlet, M., Forny, L., Meunier, V., & Zhou, W. (2023). Physical stability of co-freeze-dried powders made from NaCl and maltodextrins–impact of NaCl on glass transition temperature, water vapour sorption isotherm and water vapour sorption kinetics. *Food Hydrocolloids, 136*, Article 108238. https://doi.org/10.1016/j.foodhyd.2022.108238

Sergius-Ronot, M., Suwal, S., Pitino, M. A., Shama, S., Unger, S., O'Connor, D. L., … Doyen, A. (2023). Development of a human milk protein concentrate from donor milk: Impact of the pasteurization method on static in vitro digestion in a preterm newborn model. *Food Research International, 164*. https://doi.org/10.1016/j.foodres.2022.112385

Türker, M., Selimoğlu, S. M., & Taşpınar-Demir, H. (2022). Chapter 12—Waste(water) to feed protein: Effluent characteristics, protein recovery, and single-cell protein production from food industry waste streams. In *Clean energy and resource recovery* (pp. 201–244). Elsevier.

Van Broekhoven, S., Oonincx, D. G., Van Huis, A., & Van Loon, J. J. (2015). Growth performance and feed conversion efficiency of three edible mealworm species (*Coleoptera: Tenebrionidae*) on diets composed of organic by-products. *Journal of Insect Physiology, 73*, 1–10. https://doi.org/10.1016/j.jinsphys.2014.12.005

Van Huis, A., Van Itterbeeck, J., Klunder, H., Mertens, E., Halloran, A., Muir, G., & Vantomme, P. (2013). *Edible insects: Future prospects for food and feed security*. Food and Agriculture Organiation of the United Nations (FAO).

Wang, Z., Li, Y., Jiang, L., Qi, B., & Zhou, L. (2014). Relationship between secondary structure and surface hydrophobicity of soybean protein isolate subjected to heat treatment. *Journal of Chemistry*. https://doi.org/10.1155/2014/475389

Wilkinson, J. M. (2011). Re-defining efficiency of feed use by livestock. *Animal, 5*(7), 1014–1022. https://doi.org/10.1017/S175173111100005X

Yi, L., Lakemond, C. M., Sagis, L. M. C., Eisner-Schadler, V., Van Huis, A., & Van Boekel, M. A. J. S. (2013). Extraction and characterisation of protein fractions from five insect species. *Food Chemistry, 141*, 3341–3348. https://doi.org/10.1016/j.foodchem.2013.05.115

Yi, L., Van Boekel, M. A. J. S., Boeren, S., & Lakemond, C. M. M. (2016). Protein identification and in vitro digestion of fractions from *Tenebrio molitor*. *European Food Research and Technology, 242*(8), 1285–1297. https://doi.org/10.1007/s00217-015-2632-6

Zielińska, E. (2022). Evaluating the functional characteristics of certain insect flours (non-defatted/defatted flour) and their protein preparations. *Molecules, 27*(6339). https://doi.org/10.3390/molecules27196339

Zielińska, E., Karas, M., & Baraniak, B. (2018). Comparison of functional properties of edible insects and protein preparations thereof. *Food Science and Technology, 91*, 168–174. https://doi.org/10.1016/j.lwt.2018.01.058